Available online at www.sciencedirect.com
ScienceDirect
Journal of the European Ceramic Society 27 (2007) 3377–3384
www.elsevier.com/locate/jeurceramsoc

High-temperature deformation behavior in $SrTiO_3$ ceramics

D. Singh [a,*], M. Lorenzo-Martín [a], G. Chen [a], F. Gutiérrez-Mora [b], J.L. Routbort [a]

[a] *Argonne National Laboratory, Argonne, IL 60439, USA*
[b] *Departmento de Fisica de la Materia Condensada, Universidad de Sevilla, Sevilla 41080, Spain*

Available online 29 March 2007

Abstract

The high-temperature deformation behavior of a polycrystalline strontium titanate ($SrTiO_3$) ceramic (6 μm grain size) was investigated at temperatures of 1200–1345 °C in an argon atmosphere. Compressive deformation tests were conducted at strain rates ranging from 5×10^{-6} to 5×10^{-5} s^{-1}. Steady-state flow stresses were 0.05–30 MPa and increased with increasing strain rates. Stress exponents of ≈1, at temperatures >1200 °C, indicated a viscous diffusion-controlled deformation with an activation energy of ≈628 ± 24 kJ/mol. Comparison of activation energy with literature data suggests diffusion of cations as the rate-controlling mechanism. Absence of cavitation and grain-shape changes were consistent with grain-boundary sliding as the principal deformation mechanism. The electron back-scattered diffraction (EBSD) technique was used to determine the grain orientation as a function of applied strain. The results indicate that some of the grains rotate with cumulative rotation as large as 7° at a strain of 4%.

Keywords: Grain boundaries; $SrTiO_3$; Deformation

1. Introduction

Study of the high-temperature deformation behavior of polycrystalline ceramics is important from several perspectives: (a) high-temperature structural applications of the ceramic,[1] (b) fabrication of the ceramics with improved properties,[1–3] and recently, (c) joining of polycrystalline ceramics by plastic deformation.[4–6] In general, high-temperature deformation of polycrystalline ceramic materials, with equiaxed grains, occurs by a diffusion-controlled mechanism involving grain-boundary sliding (GBS).[7,8] It is expected that if cavitation and change in grain shape do not occur, then the grains must rotate to accommodate the deformation strains.[9]

Grain rotation during high-temperature deformation has implications in processing of ceramic materials with enhanced mechanical properties as well as in joining of ceramics. It is possible that minimizing grain boundary sliding and rotation could enhance the creep resistance of a material. Recently, various ceramics and intermetallics have been joined by high-temperature plastic deformation, which results in interfaces that are indistinguishable from the bulk material.[4–6,8,10] This joining technique operates by interpenetration of grains at joining surfaces as a result of GBS and grain rotation. No known experimental studies have quantified grain rotation in polycrystalline ceramics as a function of deformation strains. Thus, a high-temperature deformation study has been conducted on a model material, strontium titanate ($SrTiO_3$). Dense polycrystalline $SrTiO_3$ can be fabricated with relative ease and easily deformed.

Polycrystalline perovskite materials such as $BaTiO_3$ and $SrTiO_3$ have applications as capacitor materials because of their ferroelectric behavior.[11] Moreover, the earth's lower mantle is primarily composed of perovskites, namely, $(Mg,Fe)SiO_3$ and understanding its plastic deformation behavior is important.[12] The high-temperature deformation behavior of $BaTiO_3$ has been extensively studied. Park et al.[13] studied the high-temperature (1200–1300 °C) compressive deformation of polycrystalline $BaTiO_3$ with fairly large grain sizes, 19–52 μm. Their data indicated a stress exponent of 1 and activation energy of 720 kJ/mol. Moreover, Park et al. concluded that the dominant deformation mechanism was GBS assisted by lattice cation diffusion. Fine-grained (0.45 μm) $BaTiO_3$ has been deformed superplastically at 1150–1250 °C, with an activation energy of 800–1200 kJ/mol.[14]

Literature data on the high-temperature deformation of $SrTiO_3$ are fairly limited, with most of the studies conducted on

* Corresponding author at: Argonne National Laboratory, Nuclear Engineering Division, Bldg. 212/E206, 9700 S. Cass Avenue, Argonne, IL 60439, USA. Tel.: +1 630 252 5009; fax: +1 630 252 2785.
E-mail address: dsingh@anl.gov (D. Singh).

0955-2219/$ – see front matter © 2007 Elsevier Ltd. All rights reserved.
doi:10.1016/j.jeurceramsoc.2007.02.186

single crystals. Using compressive tests on $SrTiO_3$ single crystals at 1200–1520 °C, Wang et al.[12] showed power-law creep behavior in $SrTiO_3$ for samples compressed in the ⟨1 0 0⟩ and ⟨1 1 0⟩ directions. Creep along the ⟨1 1 0⟩ direction was much easier than the ⟨1 0 0⟩ direction. The stress exponent (n) was ≈3.5, and the activation energy (Q) ranged from 620 kJ/mol for the ⟨1 1 0⟩ samples to ≈750 kJ/mol for the ⟨1 0 0⟩ samples. For the case of the ⟨1 0 0⟩ samples, Q was a function of stress and/or temperature.

In this study we first investigated the high-temperature compressive deformation behavior of polycrystalline $SrTiO_3$ at various strain rates in the temperature range 1200–1345 °C. Creep deformation data and electron microscopy were used to ascertain whether GBS was the dominant deformation mechanism. Subsequently, the electron back-scattered diffraction technique was used to measure grain rotation as a function of applied plastic strain. Measured grain rotations were compared with a simulation discussed in the literature.[15]

2. Experimental details

2.1. Specimen fabrication

The $SrTiO_3$ specimens were fabricated using commercially available 98.5%-pure $SrTiO_3$ powder (#72117, Alfa Aesar, Ward Hill, MA). The $SrTiO_3$ powder compacts were formed by uniaxial pressing (45 kN force) using a hydraulic laboratory press (Carver Laboratory, Menominee Falls, WI) in a cylindrical hardened steel die. The die formed pellets of 2.2-cm diameter and 2.54-cm length. No binders were added to the powders prior to pressing.

The specimens were fired in a box furnace (Lindberg Furnaces, Asheville, NC) at 1450 °C in air for 5 h. The heating rate averaged 3 °C/min, and the cooling rate was approximately 4 °C/min.

2.2. Specimen characterization

The density of the sintered $SrTiO_3$ sample was determined by the Archimedes method. Sample preparation for microstructural examination involved polishing one of the sample surfaces down to a 0.5-μm finish using alumina slurry. To reveal grain boundaries, samples were thermally etched at 1200 °C for 0.5 h in air. Subsequently, the microstructure was examined in a Hitachi S-4700-II (Tokyo, Japan) field emission scanning electron microscope (FE-SEM). Grain size was measured by the standard linear intercept method[16] using at least 250 intercepts on SEM photomicrographs. Fabricated $SrTiO_3$ samples were analyzed by inductively coupled plasma-atomic emission spectroscopy (ICP-AES) at Argonne's Analytical Chemistry Laboratory to determine the ratio of Sr to Ti.

2.3. Deformation study

Samples for high-temperature mechanical testing were cut, ground, and polished to ≈4 mm × 5 mm × 7 mm parallelepipeds. Constant crosshead-displacement-rate experiments were carried out in an Instron machine (Model 1125, Canton, MA) equipped with an atmosphere-controlled high-temperature furnace. Details of the experimental set-up are described elsewhere.[6] The samples were compressed between two alumina platens, with platinum foil used as a diffusion barrier. Temperatures of 1200–1345 °C were used, with initial strain rates between 2×10^{-6} and 5×10^{-5} s^{-1}. Prior to start of the experiment, the chamber was back-filled and flushed with Ar gas at least three times. All experiments were conducted in ≈1 atm of high-purity (99.999%) argon atmosphere. At a specific test temperature, for each specimen, crosshead speeds were changed (with and without unloading the sample) to obtain various nominal strain rates. Strain rates were changed only after a steady state (no work hardening) was reached on the load-time trace.

Microstructural analyses of pre- and post-deformed samples were further conducted using SEM and transmission electron microscopy (TEM). TEM foils of samples were prepared by slicing thin sections with a precision diamond saw. Mechanical polishing further thinned samples. Subsequently, samples were ion milled using a Gatan (Pleasanton, CA) Model 691 precision ion polishing system. The microstructural analysis was performed with a Philips CM-200 transmission electron microscope operating at 200 kV in the Electron Microscopy Collaborative Research Center at Argonne National Laboratory.

2.4. Grain rotation measurements

Quantitative rotations of specific surface grains, as a function of applied strain, were measured using the electron backscatter diffraction (EBSD) technique.[17] A parallelepiped-shaped $SrTiO_3$ sample, with dimensions similar to the deformation study samples, was used. However, in this case, one of the four faces (parallel to the loading direction) was polished to a 0.05 μm finish using an alumina polishing solution and plasma cleaned. A small Vicker's indent was made approximately in the center of the polished face. This indentation provided a reference point so that the grains that were followed as a function of strain could be easily located. Subsequently, the polished surface was coated with a thin layer of carbon.

Electron back-scattered diffraction patterns from the $SrTiO_3$ sample were obtained with a field emission electron microscope (Hitachi S-4500, Tokyo, Japan) equipped with an orientation imaging microscopy (TSL, Draper, UT) feature at Northwestern University's Electron Probe Instrumentation Center. A special sample holder was designed so that the sample orientation in the microscope was always kept the same. Sample tilt with respect to the horizontal was 70°. Diffraction patterns or Kikuchi bands were recorded from ≈20 specific grains. To determine the grain rotation, Hough transform was used to represent the Kikuchi bands by spots.[18] The principle of the Hough transform is that the intensity at a *point* in the Hough space represents the intensity along a *line* in the original image. The coordinates in Hough space are usually taken as ρ and θ. Here, a point (ρ, θ) in the Hough transform represents a line at an angle θ and at a distance ρ from the center of the original pattern. Thus, any rotation in the grains will rotate the Kikuchi bands and spots. Grain rotation was determined by the shift in the position of the spots in the

θ coordinate in the 2D the Hough image as a function of the applied strain. If we assume the uncertainty of θ in the Hough transformed image is ± 1 pixel, the uncertainty in the rotation of the Kikuchi line (and the grain) in the original image will be $\pm 1^\circ$. This procedure is automated in the microscope and was individually applied to all the identified grains.

Grain rotation measurement, as a function of applied strain, was conducted by an interrupted test procedure. After identifying and indexing ≈20 grains on the undeformed sample, it was plastically deformed in steps of 0.02 strain at 1280 °C and a strain rate of $5 \times 10^{-6}\ s^{-1}$. At each step, the sample was removed from the Instron and placed back in the SEM to collect EBSD patterns from the identified grains. This procedure was repeated until the cumulative plastic strain in the sample was 0.08. In addition to tracking the changes in the grain orientation with deformation strains, the form factor ((4π grain area)/(grain diameter)^2) of the individual grains was tracked with strain. The form factor was determined by using standard imaging software on the SEM image of the specific grain.

3. Results

The density of the as-fabricated $SrTiO_3$ sample was ≈95% of theoretical. Fig. 1 shows the microstructure of the as-fabricated $SrTiO_3$ sample. The grains were relatively equiaxed with few entrapped pores. Average grain size was ≈6 μm. Also, since $SrTiO_3$ is soft, some polishing-related grain pullout can be seen.

Table 1 shows the results from the ICP-AES analysis. Major impurities were Zr, Si, Ba, Al, and Ca. Based purely on the weight fractions of Sr and Ti, the sintered ceramic would appear to be deficient in Ti, with a Sr/Ti atomic ratio of 1.015. Zirconium is the major impurity in the $SrTiO_3$ sample.

A typical stress–strain profile obtained under compression at 1250 °C is presented in Fig. 2. For the most part, at each strain rate, the stress reached a steady-state value. Similar responses were obtained in deformation tests conducted at other test temperatures. However, at the highest strain rate of $10^{-4}\ s^{-1}$, there was some evidence of work hardening at 1200 °C. In such cases, the stress at which plastic deformation was observed was taken as the flow stress.

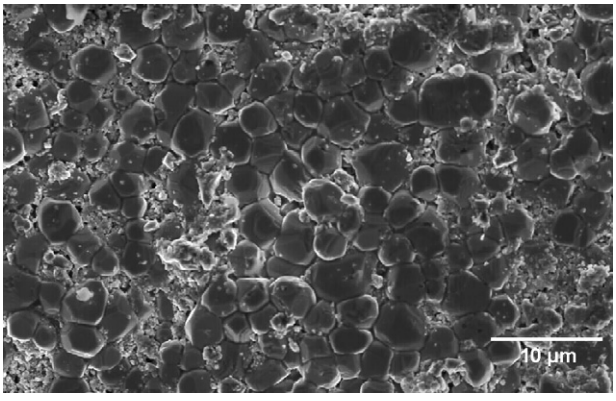

Fig. 1. SEM photomicrograph of polished and thermally etched as-fabricated $SrTiO_3$.

Table 1
ICP-AES elemental analysis of fabricated $SrTiO_3$ samples

Metal	wt.%
Sr	41.2
Ti	22.2
Zr	3.89
Si	1.45
Ba	0.79
Al	0.27
Ca	0.28
Na	0.25
Pb	<0.05
Fe	<0.05
Cu	<0.05

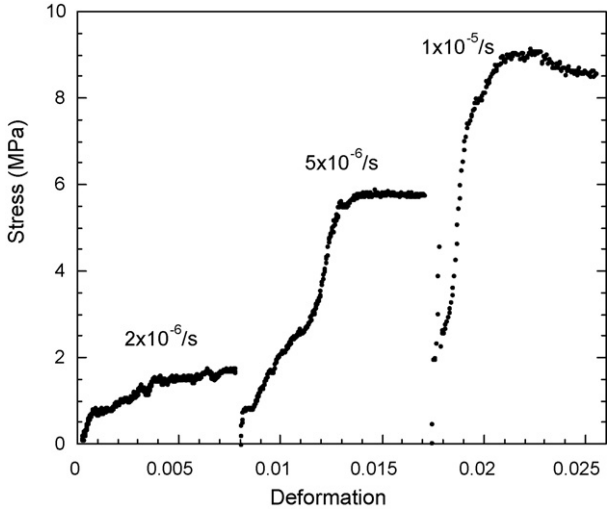

Fig. 2. Stress-deformation profile for $SrTiO_3$ obtained during compression testing at 1250 °C.

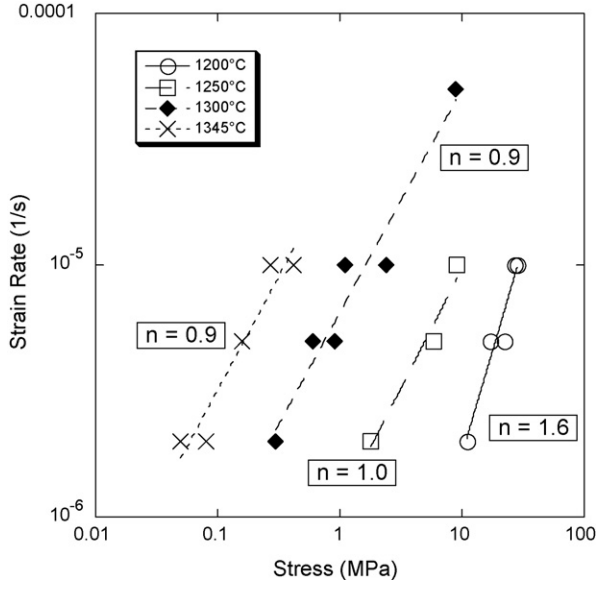

Fig. 3. Strain-rate dependency on flow stress for $SrTiO_3$ samples at various test temperatures.

Fig. 3 represents the strain-rate dependence of the flow stress for the four temperatures investigated. Assuming no substantive changes occurred in the microstructures during testing, a steady-state phenomenological creep equation can be used to define the dependence of strain rate on the flow stress[19]:

$$\dot{\varepsilon} = A\sigma^n \exp\left(-\frac{Q}{RT}\right) \quad (1)$$

where $\dot{\varepsilon}$ is the strain rate, σ the flow stress, n the stress exponent, A is a constant, Q the activation energy, R the gas constant, and T is the absolute test temperature. A stress exponent of $n = 1$ indicates that diffusion-controlled viscous flow is the likely deformation process.[1] Values of n, estimated from best fits of the experimental data in Fig. 3 to Eq. (1) were 0.9 ± 0.1 at 1345 °C, 0.9 ± 0.1 at 1300 °C, 1.0 ± 0.1 at 1250 °C, and 1.6 ± 0.1 at 1200 °C. Thus, within the experimental uncertainties in the stress and strain rates, $n = 1$ for the test temperatures between 1250 and 1345 °C.

At a constant strain rate, the activation energy, Q, for the deformation process can be represented as

$$Q = nR\left(\frac{\partial \ln \sigma}{\partial(1/T)}\right)_{\dot{\varepsilon}} \quad (2)$$

Fig. 4 shows the Arrhenius plot of flow stress as a function of reciprocal absolute temperature at the four strain rates tested. Data for tests conducted at temperatures of 1250–1345 °C were considered. From the slopes of the various lines, the mean activation energy determined was 628 ± 24 kJ/mol. It is assumed that the stress exponent, n, is constant over the temperature range. A value of $n = 1$ was used for the calculation.

Figs. 5 and 6 are typical SEM and TEM micrographs, respectively, of a $SrTiO_3$ sample that was deformed at 1350 °C with the total strain of 5%. Clearly, the grain boundaries in both photomicrographs are clean, with no cavitation or discernible changes in the grain shape observed. However, some native porosity can be seen. In addition, the TEM micrograph shows no dislocations in the deformed sample. However, the deformed samples do show evidence of twins within the grains.

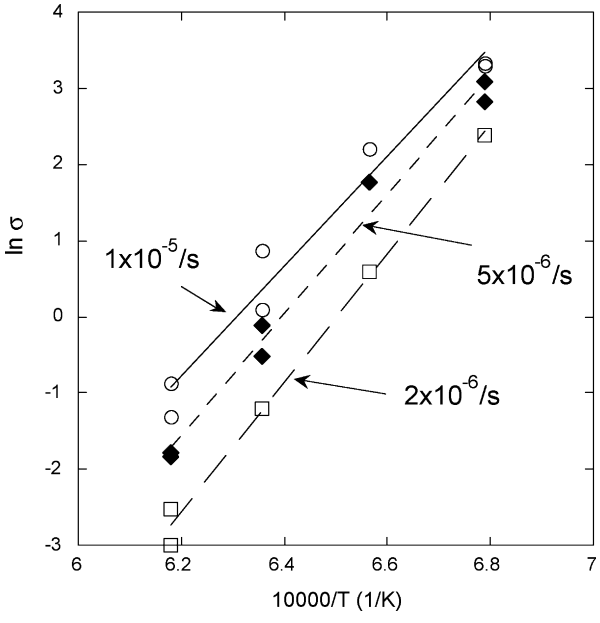

Fig. 4. Flow stress in $SrTiO_3$ as a function of test temperature at constant strain rates.

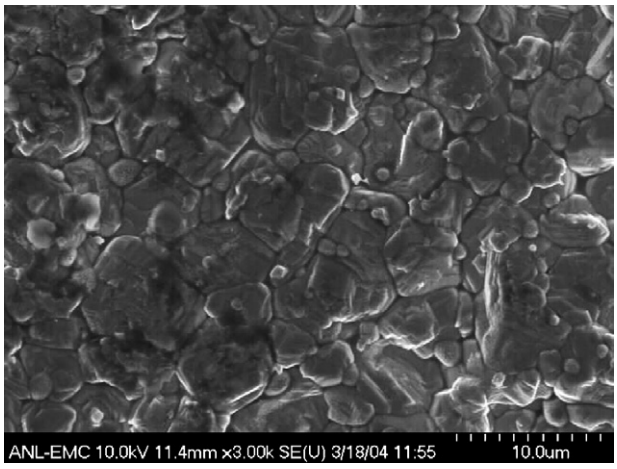

Fig. 5. SEM micrograph of $SrTiO_3$ deformed at 1350 °C to $e = 0.05$.

Fig. 7a–c present micrographs of a particular grain (#24) at strains of 0.02, 0.04, and 0.06, respectively. These micrographs demonstrate that grain (#24) can be located and tracked in the interrupted loading experiment for grain rotation measurements. It is clear from these images that no discernible change in the shape of the grain occurs with increased strain. These figures also show the diffraction patterns and their respective Hough transformed images. The rotation of a grain is detected by the shift in the spots in the Hough space. As shown in Fig. 7a and b, the spot moved by 4 pixels (from 64 to 68), or the grain rotated

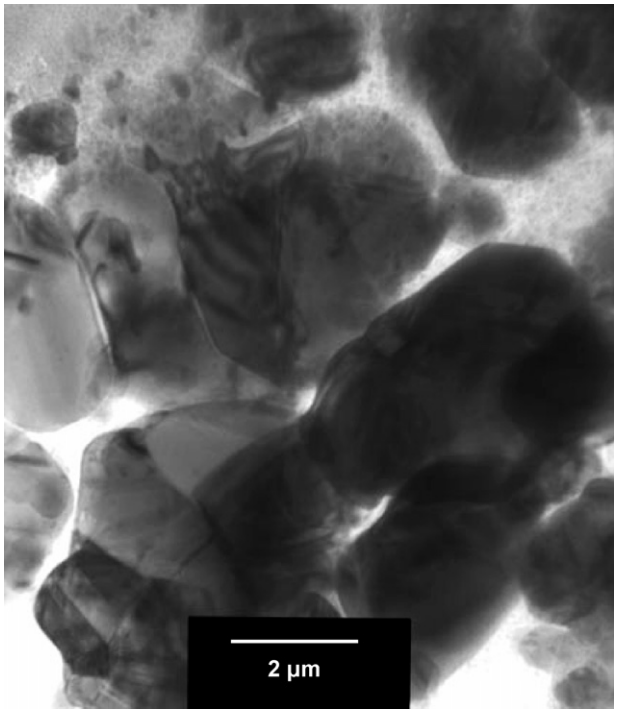

Fig. 6. TEM micrograph of $SrTiO_3$ deformed at 1350 °C to $e = 0.05$.

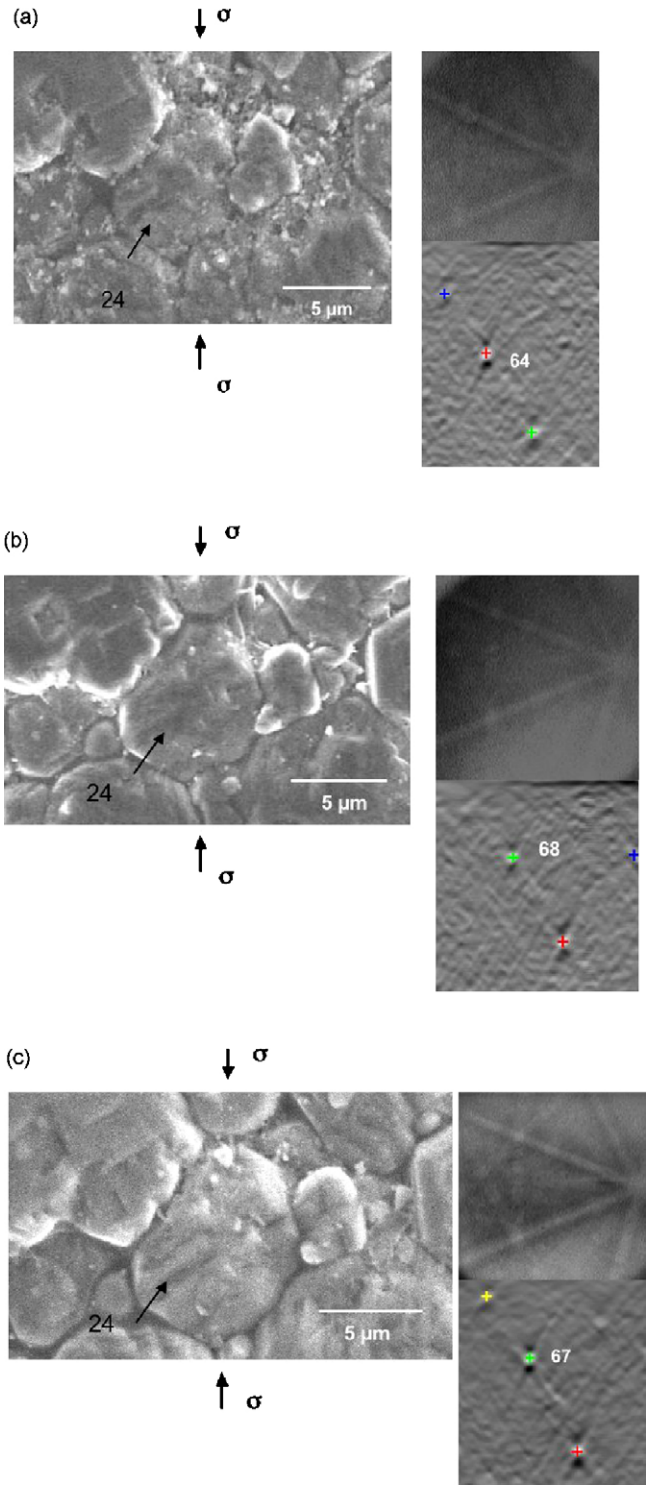

Fig. 7. SEM micrograph, diffractions bands, and corresponding Hough transforms for a specific grain deformed to (a) 2%, (b) 4%, and (c) 6% strains.

by 4° as the cumulative strain in the sample was increased from 0.02 to 0.04. Subsequently, from 0.04 to 0.06 strain, the spot shifted by 1 pixel, or the corresponding additional grain rotation was ≈1°.

Fig. 8 shows the measurable grain rotations, as a function of strain, on 7 grains out of the ≈20 grains that were followed.

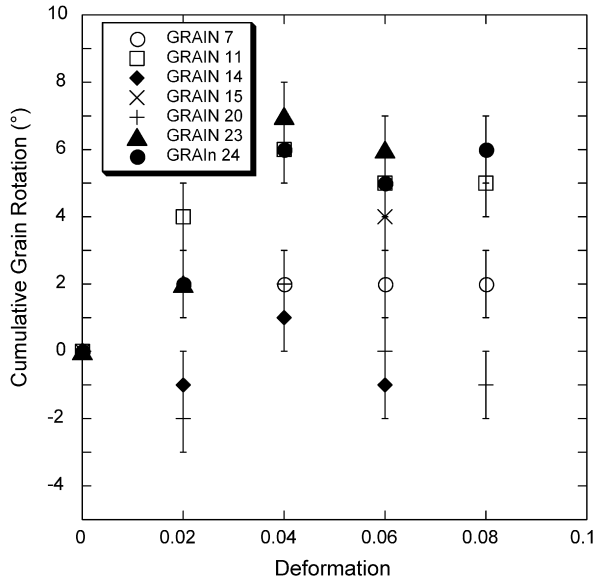

Fig. 8. Cumulative grain rotations as a function of applied strain measured on seven grains in $SrTiO_3$ deformed at 1280 °C and 5×10^{-6} s^{-1}.

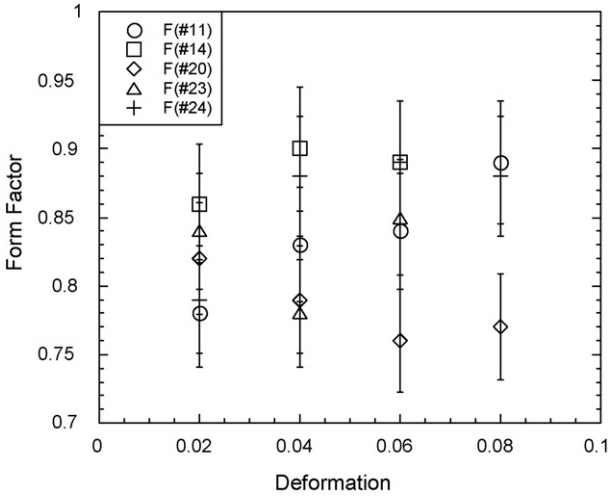

Fig. 9. Form factors of various grains as a function of plastic deformation.

These grains rotate in positive and negative directions with no systematic trend in grain rotation with the applied strain. The maximum rotation measured was 7°. Furthermore, some grains showed immediate rotation at low applied strains and then either did not rotate further or rotated back with increasing strains. Form factors measured on some of these grains as a function of applied strain are shown in Fig. 9. They do not significantly change, within the error of measurement of ±5%, which is indicative of no obvious change in grain shape.

4. Discussion

Polycrystalline $SrTiO_3$ has been shown to deform in a plastic manner at temperatures >1200 °C and strain rates as high as 1×10^{-5} s^{-1}. This behavior is analogous to the high-temperature deformation in other polycrystalline ceramics and composites, such as Al_2O_3,[20] 3Y-TZP (3 mol% Y_2O_3-stabilized

tetragonal zirconia),[2] and ceramic matrix composites.[3] It is generally accepted that deformation or plastic flow occurs in these materials by diffusion-assisted GBS.[2,3] Conditions conducive for deformation by plastic flow are met by high test temperatures, and fine and equiaxed grain structures, to accommodate the displacements of individual grains.[7]

The steady-state creep equation, Eq. (1), adequately defines the deformation behavior of $SrTiO_3$ for temperatures >1200 °C and strain rates ranging from 2×10^{-6} to 1×10^{-5} s^{-1}. A stress exponent of $n \approx 1$ is indicative of diffusion-controlled deformation process.[7] Further, absence of any deformation-induced dislocation structures in the TEM analysis (as shown in Fig. 6) indicates that $SrTiO_3$ deforms by GBS. Park et al. also observed no change in grain shapes in their study on a relatively large-grain-size (19–50 μm) $BaTiO_3$ ceramic and concluded that high-temperature deformation was controlled by GBS.[13] The stress exponent in their study was reported to be ≈1. The reason for the higher stress exponent value ($n = 1.6$) for tests on $SrTiO_3$ at 1200 °C is not clear. This higher value could be due to the onset of micro-fracture or a change in the deformation mode.

Insight into the possible deformation mechanism(s) can be gained from the activation energy measurements. The activation energy for deformation of $SrTiO_3$ ceramic was 628 ± 42 kJ/mol as determined from the Arrhenius plot of Fig. 4. This value is quite similar to the activation energy of 620 kJ/mol reported by Wang et al.[12] on creep deformation of single crystal $SrTiO_3$ deformed along the {1 0 0} ⟨0 1 0⟩ orientation. The stress exponent for single-crystal $SrTiO_3$ was 3.5, and the deformation mechanism was by diffusion-assisted-dislocation climb independent of temperature. Furthermore, Wang et al.[12] point out that this activation energy is similar to that of diffusion of Ti^{4+} ions, which are the slowest and rate-controlling species in titanate perovskites.[21,22]

For layered perovskites, such as superconductors, creep is controlled by diffusion of A site cations.[23,24] For $SrTiO_3$, the A-site cation is Sr^{2+}. The activation energy of Sr diffusion in polycrystalline $SrTiO_3$ is reported[25] to be 293 kJ/mol, which is significantly lower than the activation energy determined in the present study. It is quite possible that, in polycrystalline $SrTiO_3$, diffusion of a B-site cation or Ti^{4+} ion is the deformation controlling species because of its 4+ valence state and octahedral coordination with oxygen ions, as suggested by theoretical defect studies and experimental measurements for Ti^{4+} diffusion in titanates.[21,22] Also possible is that diffusion of the B-site cation or Ti^{4+} ion is the deformation-controlling species, as suggested by Park et al. in their work[13] on polycrystalline $BaTiO_3$. Furthermore, the role of Zr ion impurity (≈4 wt.%) in the deformation and hence, measured activation energy was not explored.

The activation energy determined for polycrystalline $SrTiO_3$ is in the range but on the lower end when compared to the activation energies of other complex-structured perovskite-type ceramics, as shown in Table 2. The normalized activation energy (Q/RT_m [R = gas constant and T_m = melting point]) allows one to compare the activation energy for various other material systems. Moreover, for these complex oxides, it is known that $n \approx 1$ and the deformation mechanism is GBS. Table 2 indicates a wide distribution in the normalized activation energies for the various perovskites.

Table 2
Activation energies for deformation of various oxide ceramics

Material	Q (kJ/mol)	Q/RT_m	Reference
$BaTiO_3$	720	46	Park et al.[13]
$CaTiO_3$	840	45	Yamada[33]
$SrZrO_3$	710	29	Nemeth et al.[34]
$SrTiO_3$ single crystal			
⟨1 0 0⟩	750	39	Wang et al.[12]
⟨1 1 0⟩	620	32	
$SrTiO_3$	628	33	This work

There are numerous examples of grain rotation during deformation, grain growth,[26] or texture evolution in metallic systems.[27] During plastic deformation, grain rotation is a consequence of a net torque on the grain.[15] However, in concert with grain rotation, an accommodating process needs to occur so that no voids or cavities are created. This accommodation is accomplished by GBS, which in the case of $SrTiO_3$ is assisted by cation diffusion.

Grain rotation in $SrTiO_3$ ceramics as a function of applied strain is clearly evident from Figs. 7 and 8. SEM and TEM images of the deformed samples show no evidence of cavitation. In addition, as shown in Fig. 9, the form factors or the grain shapes of the specific grains for which rotation was measured did not change within the accuracy of the experimental measurements. Thus, to accommodate the plastic strains, the grains have to rotate.[9] Ashby and Verrall[9] have shown that plastic strains can be accommodated by diffusion-assisted GBS that involves grain translation and rotation and little or no change in grain shape or size. Based on the Ashby–Verrall model, large strains are accommodated by neighbor-switching events, and the degree of grain rotation is dependent on the surrounding grains.[9] This model is fundamentally different from Nabarro–Herring[28] and Coble[29] creep models that predict grain shape changes with no grain rotations.

Gifkins[30] pointed out that strain rate predictions from the Ashby–Verrall model are on the lower end of the experimental measurements, and also the grain-size dependence does not agree with the experimental observations. Further, a simple two-dimensional Ashby–Verrall model does not account for the changes in the surface area. Gifkins[30] showed in his model that changes in the surface area can be accounted for by considering the grains emerging from subsurface or surface grains disappearing into the bulk. This effect was first observed and reported by Rachinger.[31] Gifkins' model[30] also predicts grain rotation.

Grains disappearing into the bulk were also evident in the present study. Fig. 10 shows a grain that was followed from 4% to 8% deformation. The grain shown by the arrow disappears into the bulk with increasing deformation. Thus, in addition to diffusion assisted GBS, there is movement of grains from the surface to interior and vice versa to account for the surface area changes as predicted by Gifkins' model.[30]

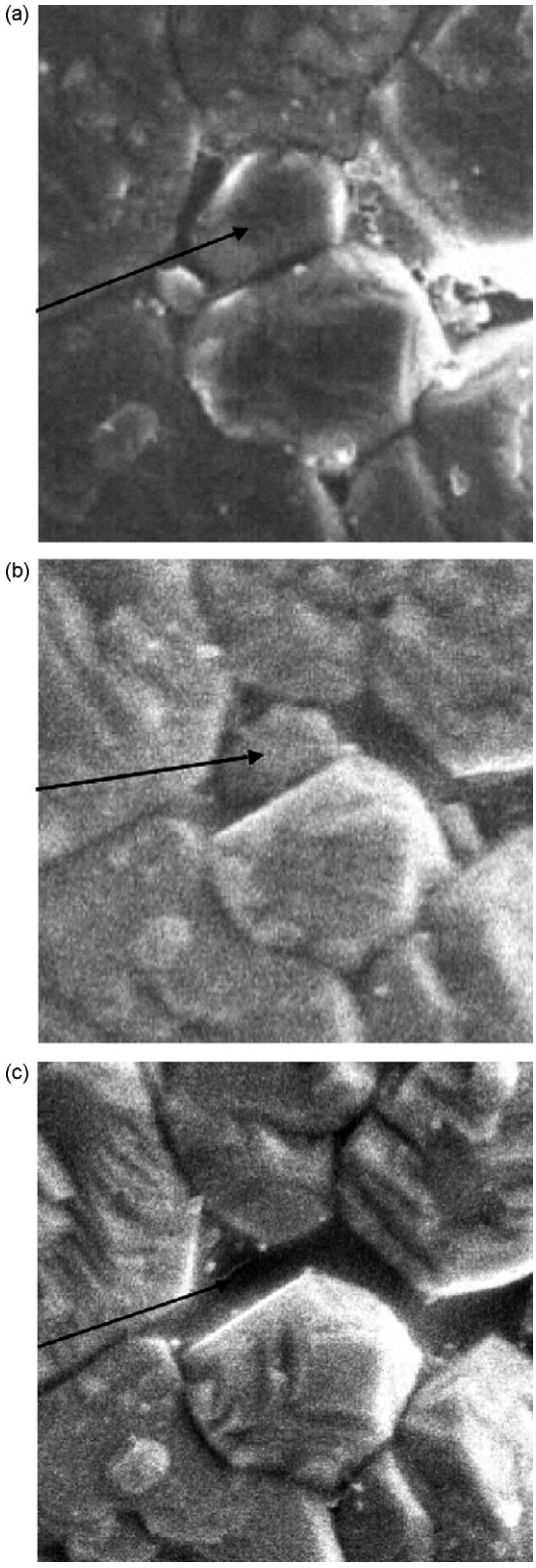

Fig. 10. Evidence of grain disappearing into the sample bulk with (a) 4%, (b) 6%, and (c) 8% deformation.

Recently, several meso-scale simulations have been performed to quantify grain rotation during plastic deformation. Notably, Ding et al.[32] have simulated grain rotation for a model material with 5000 grains. They assumed equiaxed grains with a log-normal grain size distribution and varying diffusive fluxes. However, no grain sliding resistance was considered. Deformation was accommodated by grain-boundary diffusion or Coble creep. They found that at 50% plastic strain, grain rotations ranged from -10° to $+10^\circ$, with almost 40% of the grains showing no rotation. Another 40% of the grains showed rotations between -5° and $+5^\circ$. These simulations are qualitatively similar to the experimental observations made on grain rotations as a function of plastic strain in $SrTiO_3$ in this study. It is recognized that the number of grains followed for rotation in this study is too small to provide a statistically meaningful comparison.

The grain rotation was measured in an ex-situ manner. Reloading of the specimen at each strain level is expected to create a somewhat different stress state at the microstructure level. In addition, the rotations measured are only for the surface grains. It is expected that grains in the sample interior will be exposed to different stresses and diffusion conditions. In this regard, an in situ experiment is desired where the grains in the bulk can be tracked for rotation.

5. Conclusions

Compressive deformation behavior of a polycrystalline strontium titanate ($SrTiO_3$) ceramic has been investigated at temperatures of 1200–1345 °C and strain rates ranging from 5×10^{-6} to $5 \times 10^{-5}\,s^{-1}$. Stress exponents of ≈1 indicated a viscous diffusion-controlled deformation mechanism with an activation energy of ≈628 kJ/mol. Grain boundary sliding was identified as the principal deformation mechanism. Comparison of our activation energy with literature data on single crystal $SrTiO_3$ suggests that diffusion of Ti ions is rate controlling. The electron back-scattered diffraction technique was used to determine grain orientation as a function of applied strain in $SrTiO_3$. Grain rotations were both positive and negative and as large as 7°. The magnitude of grain rotation angles was qualitatively similar to that predicted from simulations.

Acknowledgments

This work was supported by the Office of FreedomCar and Vehicle Technologies of the U.S. Department of Energy, under Contract No. DE-AC02-06CH11357 at Argonne National Laboratory, managed by University of Chicago Argonne LLC (USA). The authors are grateful to the late program manager, Dr. S. Diamond. The electron microscopy work was performed at the Electron Microscopy Collaborative Research Center at the Argonne National Laboratory and Electron Microscopy Service at the University of Sevilla.

References

1. Cannon, R. W. and Langdon, T. G., Creep of ceramics—1. Mechanical characteristics. *J. Mater. Sci.*, 1983, **8**(1), 1–50.
2. Wakai, F., Sakaguchi, S. and Matsuno, Y., Superplasticity of yttria-stabilized tetragonal zirconia. *Adv. Ceram. Mater.*, 1986, **1**, 259.
3. Chokshi, A. H., Mukherjee, A. K. and Langdon, T. G., Superplasticity in advanced materials. *Mater. Sci. Eng.*, 1993, **R10**, 237–240.

4. Ye, J. and Domínguez-Rodríguez, A., Joining of Y-TZP parts. *Scripta Metall. Mater.*, 1995, **33**, 441–446.
5. Gutierrez-Mora, F., Domínguez-Rodríguez, A., Routbort, J. L., Chaim, R. and Guiberteau, F., Joining of yttria-tetragonal stabilized zirconia polycrystals using nanocrystals. *Scripta Mater.*, 1999, **41**, 455–460.
6. Goretta, K. C., Gutiérrez-Mora, F., Picciolo, J. J. and Routbort, J. L., Joining alumina/zirconia ceramics. *Mater. Sci. Eng. A*, 2003, **341**, 158–162.
7. Langdon, T. G., The characteristics of superplastic-like flow in ceramics. In *Plastic Deformation of Ceramics*, ed. R. C. Bradt, C. A. Brookes and J. L. Routbort. Plenum Press, New York, 1995, pp. 251–268.
8. Gutiérrez-Mora, F., Goretta, K. C., Majumdar, S., Routbort, J. L., Grimdisch, M. and Domínguez-Rodríguez, A, Influence of internal residual stresses in superplastic joining of zirconia toughened alumina. *Acta Mater.*, 2002, **50**, 3475–3486.
9. Ashby, M. F. and Verrall, R. A., Diffusion-accommodated flow and superplasticity. *Acta Metall.*, 1973, 149–163.
10. Singh, D., Gutierrez-Mora, F., Chen, N., Goretta, K. C. and Routbort, J. L., Joining of advanced materials by plastic deformation. *Ceram. Eng. Sci.*, 2004, **25**(3), 113–119.
11. Jona, F. and Shirane, G., *Ferroelectric Crystals*. Dover, New York, 1993.
12. Wang, Z., Karato, S. and Fujino, K., High temperature creep of single crystal strontium titanate ($SrTiO_3$): a contribution to creep systematics in perovskites. *Phys. Earth Planet. Int.*, 1993, **79**, 299–312.
13. Park, E. T., Nash, P., Wolfenstine, J., Goretta, K. C. and Routbort, J. L., High-temperature creep of polycrystalline $BaTiO_3$. *J. Mater. Res.*, 1999, **14**(2), 523–528.
14. Carry, C. and Mocellin, A., Superplastic creep of fine-grained $BaTiO_3$ in a reducing environment. *J. Am. Ceram. Soc.*, 1986, **69**, C215–C216.
15. Moldovan, D., Wolf, D. and Phillpot, S. R., Theory of diffusion-accommodated grain rotation in columnar polycrystalline microstructures. *Acta Mater.*, 2001, **49**, 3521–3532.
16. Underwood, E. E., *Quantitative Stereology*. Addison-Wesley Pub. Co., Reading, MA, USA, 1970.
17. Humphreys, F. J., Review: grain and subgrain characterisation by electron backscatter diffraction. *J. Mater. Sci.*, 2001, **36**, 3833–3854.
18. Tao, X. and Eades, A., Errors, artifacts, and improvements in EBSD processing and mapping. *Microsc. Microanal.*, 2005, **11**, 79–87.
19. Bretheau, T., Castaing, J., Rabier, J. and Veyssiere, P., Dislocation motion and high-temperature plasticity of binary and ternary oxides. *Adv. Phys.*, 1979, **28**, 835–865.
20. Xue, L. A. and Chen, I. W., Deformation and grain growth of low-temperature-sintered high-purity alumina. *J. Am. Ceram. Soc.*, 1990, **72**, 3518–3522.
21. Rhodes, W. H. and Kingery, W. D., Dislocation dependence of cationic diffusion in $SrTiO_3$. *J. Am. Ceram. Soc.*, 1996, **49**(10), 521–526.
22. Wright, K. Rheology of perovskites and its implications for mantle dynamics. Ph.D. Thesis. Department of Geological Science, University College, London, United Kingdom, 1991.
23. Domínguez-Rodríguez, A., Castaing, J., Goretta, K. C. and Routbort, J. L., In *Point Defects and Related Properties of Ceramics*, ed. T. O. Mason and J. L. Routbort. Am. Ceram. Soc., Westerville, OH, USA, 1991, p. 139.
24. Jiménez-Melendo, M., Domínguez-Rodríguez, A., Goretta, K. C. and Routbort, J. L., Diffusion-controlled plastic deformation of $YBa_2Cu_3O_x$. *Acta Metall. Mater.*, 1995, **43**, 2429–2431.
25. Turlier, P., Bussiere, P. and Prettre, M., *Comp. Rend. Acad. Sci.*, 1960, **250**, 1649.
26. Shewmon, P. G., *Recrystallization Grain Growth and Textures*. American Society for Metals, Metals Park, OH, USA, 1966.
27. Yamaskai, T., Demizu, Y. and Ogino, Y., *Mater. Sci. Forum*, 1996, **461**, 204–206.
28. Herring, C., Diffusional viscosity of a polycrystalline solid. *J. Appl. Phys.*, 1950, **21**, 437–439.
29. Coble, R. L., A model for boundary diffusion controlled creep in polycrystalline materials. *J. Appl. Phys.*, 1963, **34**, 1679–1681.
30. Gifkins, R. C., Grain rearrangements during superplastic deformation. *J. Mater. Sci.*, 1978, **13**, 1926–1936.
31. Rachinger, W. A., *J. Inst. Met.*, 1952/1953, **81**, 33.
32. Ding, R., Moldovan, D., Yamakov, V., Wolf, D. and Phillpot, S. R., Effects of microstructural inhomogeneity on dynamic grain growth during large-strain grain boundary diffusion-assisted plastic deformation. *Model. Simul. Mater. Sci. Eng.*, 2005, **13**, 1129–1151.
33. Yamada, H., Viscous creep deformation of polycrystalline $CaTiO_3$ at elevated temperatures. *J. Mater. Sci.*, 1984, **19**, 2639–2642.
34. Nemeth, J., Youdelis, W. V. and Parr, J. G., High-temperature creep behavior of polycrystalline $SrZrO_3$. *J. Am. Ceram. Soc.*, 1972, **55**, 125–129.